

Observed variability in the upper layers at the Equator, 90°E in the Indian Ocean during 2001–2008, 2: meridional currents

R. R. Rao¹ · T. Horii² · Y. Masumoto^{2,3} · K. Mizuno²

Received: 18 May 2015 / Accepted: 4 January 2016 / Published online: 24 February 2016
© Springer-Verlag Berlin Heidelberg 2016

Abstract In the Indian Ocean, the observed variability of meridional currents (MC) at the Equator, 90°E shows distinct 10–20 day (quasi-biweekly) north–south reversals in the near-surface 40–350 m water column. Unlike the zonal currents, the seasonal variability in the MC field is strikingly absent in the annual cycle over this water column. However, the strong amplitude oscillations penetrate deep during boreal winter, boreal spring and boreal fall seasons. There is also a suggestion that they are weak and shallow during summer monsoon season during the years when the intraseasonal zonal westerly wind bursts along the equator are weak or absent. These quasi-biweekly oscillations are attributed to the westward propagating equatorially trapped mixed Rossby-gravity (MRG) or Yanai waves triggered by the westward propagating meridional wind (MW) field along the equator suggesting a possibility of wind-forced response of the upper ocean. A careful examination reveals interannual modulation of this quasi-biweekly variability in the MC field. The salinity induced vertical stratification observed in the near-surface layer through barrier layer effects also shows a significant influence on the MC field on 10–20 day time scale. The upwelling and downwelling

cycles caused in the near off-equatorial region as a result of the westward propagation of the MRG waves are noticed in the pycnocline inferred from the vertical temperature and salinity profiles recorded by a nearby TRITON CTD mooring deployed at 1.5°S, 90°E. The observed sharp differences in the MCs between years appear to be determined by the strengths of both MWs and barrier layer thickness. A suggestion of westward propagation of quasi-biweekly variability in SST along the equator with phase speed resembling that of the MRG waves is also episodically seen during most years.

Keywords Meridional currents · Equator, 90°E · Indian Ocean · Intraseasonal variability · Interannual variability

1 Introduction

The measurements of horizontal currents made in the tropical Indian Ocean (TIO) although few, show rich temporal variability not only on seasonal time scale but also on intraseasonal and interannual time scales (Schott and McCreary 2001; Schott et al. 2009). The first direct current measurements made near the Gan Island in the central equatorial Indian Ocean (EIO) during 1973–1974 have suggested variability of the currents with periods shorter than 20 days in addition to strong zonal currents (ZCs) at semiannual frequency associated with Wyrтки jets (Wyrтки 1973, Knox 1976 and McPhaden 1982). Luyten and Roemmich (1982) have also found a strong signal in the 200 m deep MC spectrum of the data collected during April, 1979–June, 1980, with a peak at 26 days, that is not observed in the ZCs in the western EIO. This result is attributed to the mixed Rossby-gravity (MRG) waves (or Yanai waves). The zonal wavelength of this oscillation is estimated to be approximately

This paper is a contribution to the special issue on Ocean estimation from an ensemble of global ocean reanalyses, consisting of papers from the Ocean Reanalyses Intercomparison Project (ORAIP), coordinated by CLIVAR-GSOP and GODAE OceanView. The special issue also contains specific studies using single reanalysis systems.

✉ R. R. Rao
rokkamr@yahoo.com

¹ IITM, Pune, India

² JAMSTEC, Yokosuka, Japan

³ University of Tokyo, Tokyo, Japan

1100–2000 km, with meridional velocities of 15–30 cm/s (Reverdin and Luyten 1986; Tsai et al. 1992). In addition, these oscillations show a westward propagation along the equator, with eastward and downward energy propagation. But the phase can travel eastward or westward depending on the frequency. In the central EIO, south of Sri Lanka, the direct current measurements made by Schott et al. (1994) during January, 1991–February, 1992 have also suggested the occurrence of oscillations of 10–20 day (quasi-biweekly) periods. South of Sri Lanka along 80.5°E, the ZC and upper-ocean zonal volume transports in the off-equatorial region from a meridional array of Acoustic Doppler Current Profilers (ADCPs) and Rotor Current Meters (RCMs) have also shown large fluctuations at quasi-biweekly period. The subsequent direct current measurements made along 80.5°E during July, 1993–September, 1994 further confirmed the occurrence of 15 day spectral peak both in the equatorial MC and off-equatorial ZC (Rep-pin et al. 1999) in agreement with the meridional structure of the wind forced MRG waves (Matsuno 1966; Gill 1982). In an OGCM simulation, Sengupta et al. (2001) have also shown that the intraseasonal fluctuations in the zonal transport in the off-equatorial region forced by the wind stress, are associated with westward propagating MRG waves.

Understanding of MCs is important for the meridional heat and salt transport across the equator and for the shallow meridional overturning cell in the EIO (Loschnigg and Webster 2000, Miyama et al. 2003). The interannual variability in the Wyrтки Jet has significant influence on fresh water transport between the equatorial Indian Ocean and the Bay of Bengal (Thompson et al. 2006). Based on the direct current measurements made at 83°E (December, 2000–December, 2001) and at 93°E (December, 2000–March, 2002) on the equator and from an OGCM simulation, Sengupta et al. (2004) have shown the occurrence of 10–20 day (quasi-biweekly) oscillations that are distinct from long period oscillations of 20–60 days in the meridional flow. The temporal lags between these two moorings on the equator have indicated the presence of packets of westward and vertically propagating waves with zonal wave lengths in the range of 2100–6100 km. Using an OGCM, they have reported that the observed quasi-biweekly variability is due to equatorially trapped MRG waves generated by the subseasonal variability of the winds. The quasi-biweekly fluctuations of surface meridional wind (MW) stress resonantly excite MRG waves with westward and upward phase propagation, with a typical period of 14 days and zonal wavelengths of 3000–4500 km. The MW stress can trigger MRG waves as these waves are associated with symmetric MC and antisymmetric ZC fields near the equator (Wunsch and Gill 1976). These quasi-biweekly waves are associated with fluctuating upwelling/downwelling cycles in the EIO, with amplitudes of 2–3 m/day located 200–300 km

away from the equator (Sengupta et al. 2004). Based on a quick look analysis of direct measurements of ADCP currents made during November, 2000–October, 2001, by JAMSTEC (Japan Agency for Marine-Earth Science and Technology) at the same location of the present study, Masumoto et al. (2005) have also shown vertically coherent MCs with large amplitudes and periods 10–20 days in the layer shallower than 100 m. The period of maximum variability tends to shift to longer time scales in the deeper levels, with a period of nearly 30 days at the depth of 200 m. The dynamics of these quasi-biweekly oscillations of these waves in the EIO are examined both with an OGCM and continuously stratified model by Miyama et al. (2006). They have reported that the dynamics of the quasi-biweekly variability are fundamentally linear and wind driven. The quasi-biweekly response is composed of local (non-radiating) and remote (Yanai wave) parts, with the former spread roughly uniformly along the equator and the latter strengthening to the east. Both forcings contribute to the quasi-biweekly signal, the response forced by the MW stress being somewhat stronger. The MRG (Yanai) waves carry energy downward and eastward from multiple modes resulting in eastward intensification of the MCs in the EIO (Sengupta et al. 2004, Miyama et al. 2006). Analysis of RCM mooring data collected at 77°E (168 m, 2003–2004), at 83°E (141 m, 2002–2003) and at 93°E (106 m, 2002–2003) by Murty et al. (2006) has demonstrated significant intraseasonal variability in the spectra of MCs at periods between 15 and 24 days. Halkides et al. (2007) have used the Hybrid Coordinate Ocean Model of Bleck (2002) and reported that the contribution of the subseasonal variability to the meridional heat transport through shallow meridional circulations (Miyama et al. 2003 and Schott et al. 2004) on the seasonal to interannual variability in the Indian Ocean can account for 30 % in some years. Loschnigg and Webster (2000) and Waliser et al. (2004) have also suggested that wind forced intraseasonal currents make a significant contribution to ocean heat transport and upper ocean heat balance. Miyama et al. (2006) have proposed another mechanism for the generation of quasi-biweekly MC variability in the upper layers of the eastern EIO. They have found in their model simulation that the MRG wave is excited in the western EIO and a ray-path of its energy penetrates into the deep ocean and then is reflected at the bottom to reach the upper eastern EIO causing further intensification of the MCs. Ogata et al. (2008) have shown both in a high resolution model simulation and in limited ADCP measurements made during 2001 at the same location of the present study that energy peaks occur in two distinct time scales; one in the quasi-biweekly period above the thermocline and the other in the 20–70 day period in the subsurface layer. They have further shown that the quasi-biweekly current field's horizontal structure is consistent

with the MRG waves at 15 day period. This MC variability shows large coherence with the local MW stress associated with the atmospheric intraseasonal variability, suggesting the upper-ocean response to the local wind forcing.

Unlike the Atlantic and Pacific Oceans, the meridional gradient of SST in the EIO is weak due to absence of equatorial upwelling thus limiting our ability to infer the meridional displacements through remote sensing. Hence the only option would be to deploy vertical arrays of RCMs and ADCPs to record long time series of current measurements. One such pioneering effort launched by JAMSTEC through the deployment of upward looking ADCP at the Equator, 90°E as early as November, 2000 coinciding with the RAMA observational initiative has yielded a long record of time series data set. The data set available for full 8 year record (2001–2008) utilized in the present study is reliable and long enough to represent a benchmark data set for model validation on several time scales. In a companion study, Rao et al. (2015) have analyzed the same ADCP data set to describe and explain the observed variability in the ZCs at this location. In the present study, all the available full 8 year record of ADCP data are utilized to provide the comprehensive description and to explain the observed meridional flow on seasonal, intraseasonal and interannual time scales. In particular the following issues are addressed.

- The role of westward propagating MW field along the equator on the observed MC field.
- The influence of salinity induced near-surface stratification on the observed MC field.
- Observational evidence for the upwelling/downwelling in the pycnocline in association with MRG waves near the equator.
- The potential influence of the MRG waves on the westward propagation of SST variability along the equator.

2 Observations and methodology

A combination of several types of archived in situ measurements and the relevant historical satellite data are assembled and utilized in this study to describe and explain the observed variability of the MCs at the Equator, 90°E in the Indian Ocean. An upward looking ADCP was deployed by JAMSTEC around 400 m depth at this location in the Indian Ocean on 14 November, 2000 and the hourly data are available since then uninterruptedly at 8 m vertical resolution (Masumoto et al. 2005). The data above 40 m depth are not accurate due to surface reflections and hence not considered in this study. The daily averaged data set collected from November, 2000 to March, 2009 is utilized in the present study to characterize the observed variability in the north–south flow in the depth range of 40–350 m. The vertical profiles of temperature and

salinity in the topmost 750 m water column recorded by the CTD sensors attached to a TRITON buoy (Kuroda 2002) deployed by JAMSTEC at 1.5°S, 90°E since 23 October, 2001 are utilized to characterize the vertical fluctuations in the pycnocline (Hase et al. 2008) and to characterize the barrier layer thickness (BLT). As the vertical resolution of the CTD sensors of the TRITON mooring is not fine, the spline method of Akima (1970) is utilized to interpolate data in depth and in time when data were missing on very few occasions. These data are utilized to characterize the observed upwelling/downwelling cycles in the near off-equatorial regions. The QuikSCAT surface winds (Wentz et al. 2001) are utilized to assess their impact on the observed MC field and the westward propagating MRG waves. These winds and the OSCAR (Ocean Surface Current Analysis—Real time) currents (Lagerloef et al. 1999; Johnson et al. 2007) for all the available years are also utilized to characterize the basin scale variability in the spectral domain for the TIO. Shikha-kolli et al. (2013) have evaluated OSCAR surface currents in the TIO using the available in situ data. The TRMM TMI (Tropical Rainfall Measuring Mission's Microwave Imager) sea surface temperature (SST) data are utilized to characterize the quasi-biweekly westward propagation along the equator. The bandpass filtering of MC, MW, BLT, sigma-t, OLR, surface net heat flux and SST data is done following Duchon (1979). A large sample of 2048 points is considered for the estimations of power spectra and cross spectra of the MWs, MCs, BLT and sigma-t following Hino (1977). The sources, periods, accuracies and resolutions of the data sets utilized in this study are shown in Table 1.

3 Analysis

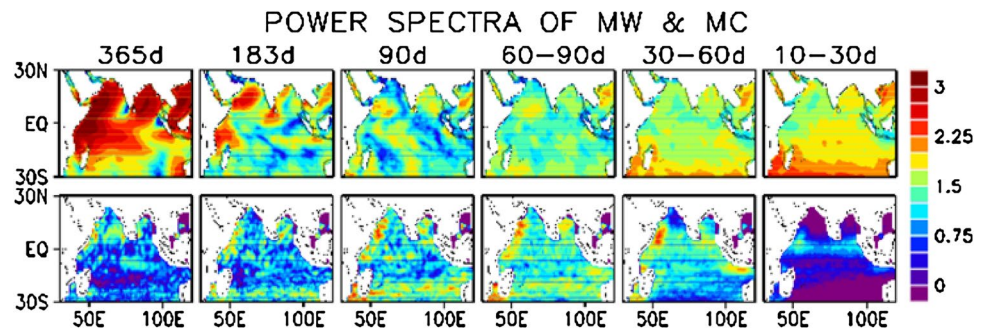
3.1 Spatio-temporal variability of MWs and MCs in the TIO

To set the background for this study, all the available historic data are utilized to construct a comprehensive framework to portray the observed spatio-temporal variability of surface MWs based on QuikSCAT surface winds and surface MCs based on OSCAR surface currents through their basin-scale variance preserving power spectral distributions. The amplitudes of power spectra for different prominent temporal modes such as annual, semiannual, 90, 60–90, 30–60, and 10–30 day are shown in Fig. 1 for the entire TIO. The spectral distribution of MWs (Fig. 1, top panel) shows strong annual mode over the western Arabian Sea, western EIO and the south central Bay of Bengal in association with the reversing seasonal monsoons. The signal clearly shows the predominance of the cross equatorial wind flow associated with the summer monsoon both in the western Indian Ocean and in the south central Bay of Bengal. The semiannual signal is

Table 1 Data sources, periods, accuracies and resolutions

Parameter	Source	Period	Accuracy	Spatio-temporal resolution
ADCP MC	JAMSTEC	November 2000–March 2009	1 % 5 mm/s	10 m in the vertical (40–350 m) and 1 day
TRITON temperature and salinity	www.jamstec.go.jp	October 2001–September 2007	0.002 °C 0.04 PSU	1.5, 25, 50, 75, 100, 125, 150, 200, 250, 300, 500, 750 m depths in the vertical and 1 day
QuikSCAT MW	www.ssmi.com	2001–2008	2 m/s	0.25° in the horizontal and 1 day
TRMM TMI SST	www.ssmi.com	2001–2008	~0.5 °C	0.25° in the horizontal and 1 day
OSCAR MC	www.dapper.pmel.noaa.gov/dapper/oscar/world-unfilter.nc	1992–2008	–	1.0° and 5 days

Fig. 1 Amplitude of variance preserving power spectra of QuikSCAT MW (*top panel*) and OSCAR MC (*bottom panel*) for the temporal modes such as annual, semiannual, 90, 60–90, 30–60, and 10–30 day for the TIO (units are arbitrary and are multiplied by appropriate scale factors for easy comparison)



also large over the western Arabian Sea and off the east coast of Africa in the latitudinal band from the Equator to 10°S, and in the region south of Indo-Sri Lanka Channel where winds reverse seasonally in association with both the monsoons (Rao et al. 2009). In general, in the TIO the amplitude of the power spectra decreases from seasonal to intraseasonal mode with the exception of southern TIO for the 10–30 day period where the influence of eastward moving extra-tropical waves could be important. At the higher frequencies, the signal is relatively stronger over the central EIO, the Bay of Bengal and southern Arabian Sea where the warm pool is located. Thus it is clear that the peak in the spectral power shifts from low frequency mode in the western basin to high frequency mode in the eastern and southern basins.

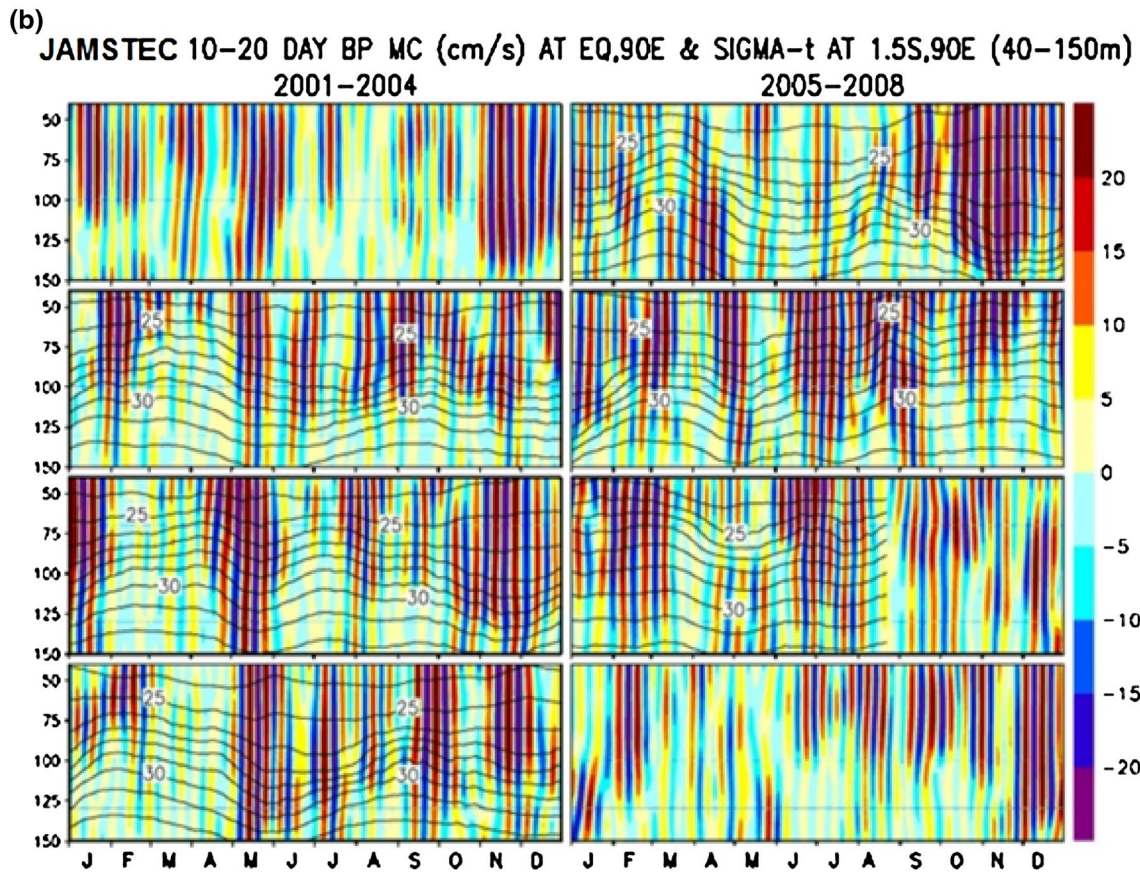
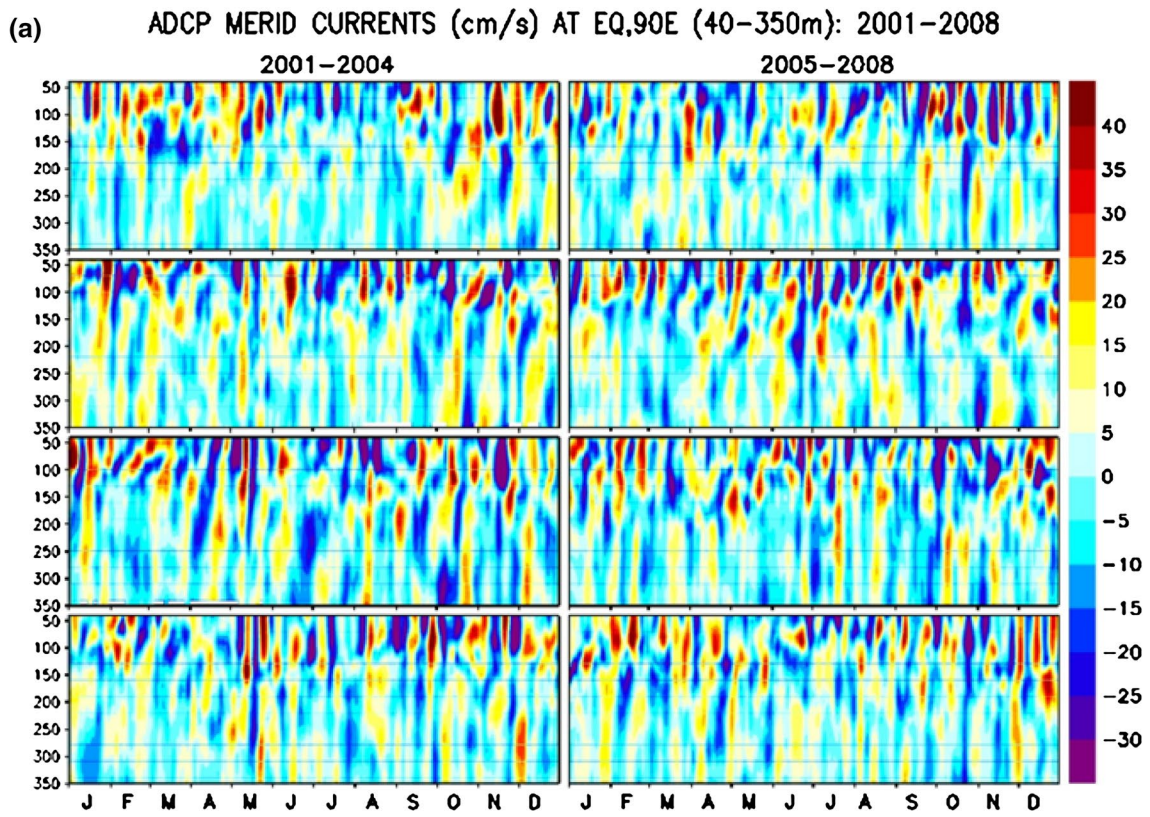
The amplitude of the power spectral distribution of MC (Fig. 1, bottom panel) shows a strong signal off the Somalia coast at all temporal modes. The instability of the western boundary currents contribute significantly to the observed variability off the Somalia coast on seasonal to intraseasonal time scales (Kindle and Thompson 1989, Sengupta et al. 2001). The power spectra corresponding to 30–90 day period is more pronounced over the northern Bay of Bengal, southeast of Sri Lanka where the warm pool is located. The power spectra corresponding to 60–90 day period is more pronounced over the southern TIO. The OGCM simulations of Sengupta et al. (2004) and of Ogata et al. (2008) have also shown large quasi-biweekly variability along the equator, with a meridional width of about four degrees in

Fig. 2 **a** Observed interannual variability of daily JAMSTEC ADCP MCs (cm/s) in the 40–350 m water column at the Equator, 90°E during 2001–2008 (years increasing downward). **b** Observed interannual variability of the 10–20 day bandpass filtered JAMSTEC ADCP MCs (cm/s) in the 40–150 m water column at the Equator, 90°E during 2001–2008 (years increasing downward) and 31 day moving-averaged sigma-t contours at 1.5°S, 90°E during 2002–2007

both the hemispheres. But the distribution of power spectral amplitude of MCs corresponding to 10–30 days in the equatorial region appears to be underestimated in view of coarse temporal resolution of OSCAR data.

3.2 Observed variability of MCs

All the processed ADCP MC data collected in the 40–350 m water column are presented for the individual years 2001–2008 (Fig. 2a). Unlike the ZCs, MCs do not exhibit any clear seasonal variability. Instead, they show complex coherent vertical structures with high frequency variability in the entire water column. The MCs are relatively stronger in the uppermost 150–200 m layer compared to those in the layer below. However, there is no evidence of current maxima occurring all the time close to the near-surface. Episodic occurrence of isolated vertically coherent subsurface current maxima is a common feature. A distinct 10–20 day (quasi-biweekly) period is most conspicuously seen throughout the 40–350 m water column.



Occurrence of alternate bands of northward and southward flowing MCs are seen throughout the year. A careful examination also reveals an interannual modulation of this quasi-biweekly variability in the MC field. The MCs show vertical phase propagation generally, but not always upward in agreement with the modeling results of Sengupta et al. (2004) and Miyama et al. (2006). Sengupta et al. (2004) have proposed that the atmospheric quasi-biweekly mode resonantly forces quasi-biweekly MRG waves in the ocean. The MCs associated with these waves also accordingly show the quasi-biweekly variability.

To get a better clarity on the observed interannual variability of the observed quasi-biweekly MCs, the MCs are bandpass filtered for 10–20 days for all the 8 years and their distributions along with sigma-t surfaces derived from a nearby location (1.5°S and 90°E) are shown in Fig. 2b. The filtering is limited to 40–150 m water column as much of the variability is limited to 150 m depth. At 10–20 day period, large interannual variability occurring as packets is clearly seen in the observations. In general, the amplitude of the variability tends to be large during boreal spring and boreal fall in tune with the depression of the pycnocline associated with the eastward flowing Wyrki jets. This relationship may be attributed to co-occurrence of strong equatorial winds, shallow mixed layer depth and thick barrier layer during boreal spring and boreal fall (Qu and Meyers 2005) favoring a strong coupling between local MWs and MCs at 10–20 day period. In addition, packets showing strong variability are also seen episodically during boreal winter and boreal summer. Distinct interannual variability in the 10–20 day bandpass filtered MC is seen during boreal spring and boreal fall seasons. Stronger (weaker) packets of MCs have occurred during boreal spring in the years 2001, 2003 and 2004 (2005, 2007 and 2008). During the boreal fall season, they are relatively stronger (weaker) during 2001, 2003 and 2005 (2002, 2006 and 2007). During the summer monsoon seasons preceding the IOD years 2006 and 2007, the MCs are unusually stronger when the corresponding MWs are also stronger (Figs. 2b, 4b). Co-occurrence of relatively stronger (weaker) MCs and MWs is seen during spring of 2003 and 2004 (2007 and 2008). During fall, the co-occurrence of relatively stronger (weaker) MCs and MWs is seen during 2003 and 2005 (2006 and 2007). The observed sharp differences in the MCs between years appear to be determined by the strengths of both MWs and BLT (Fig. 7a). The combination of thick (thin) barrier layer and strong (weak) MWs would result in strong (weak) MCs as evidenced during the spring season of 2003 (2007) and during the fall season of 2005 (2006).

3.3 Observed mean annual cycle of MCs

All the processed data collected by the ADCP mooring deployed by JAMSTEC at the Equator, 90°E in the

40–350 m water column for the years 2000–2009 are utilized to generate daily climatological mean and variance of the MC and their distributions are shown in Fig. 3. Unlike the ZC, the mean distribution of MC does not show any clear seasonal cycle in the entire water column. Instead, a complex vertical structure of alternate bands of northward and southward flowing currents at high frequency (quasi-biweekly) is seen throughout the 350 m water column. Relatively larger amplitudes are seen in the uppermost 150–200 m layer compared to the below layers. The quick look analysis of this ADCP data by Masumoto et al. (2005) during the period November 2000–October 2001 has also shown a quasi-biweekly variability in the MC field at this location in the eastern EIO. This quasi-biweekly variability is distinctly different from the other intraseasonal (20–90 days) variability. Deep penetration of isolated and strong current patches occurs episodically almost throughout the year with no apparent seasonality. Strong northward flowing currents below 100 m are seen episodically almost throughout the year. However, relatively large amplitude variability is seen during January to June and during September to December, and it is small during boreal summer as reported by Ogata et al. (2008). The lower boundary of the near-surface layer currents vertically migrates at semi-annual periodicity in response to the Wyrki jets with peaks during boreal spring and boreal fall seasons. On the other hand the variance of MCs appears to show some seasonality in the uppermost 150 m layer. It is largest during the late summer monsoon and the boreal fall transition when the ZWs are also relatively stronger. The strong variance of MCs during September–October is attributed to the observed transition from southerly winds to northerly winds (Fig. 4a). The following boreal winter months also see larger variance in the MC field.

4 Governing mechanisms

4.1 Interannual variability of MWs along the equator

It is well known that the near-surface circulation in the oceans is governed by both the local and remote wind forcings (Schott et al. 2009). Earlier modeling studies (Sengupta et al. 2004; Ogata et al. 2008) have shown strong relationship between the MWs and the westward propagating MRG waves along the equator that drive MCs in the eastern EIO. In the eastern EIO, atmospheric variability shows dominant intraseasonal fluctuations both at 30–60 day and at 10–20 day periods (Krishnamurti and Arduay 1980; Yasunari 1981; Goswami et al. 1998). The interaction between eastward propagating Madden–Julian oscillations at 30–60 day period and the westward propagating MRG waves at 10–20 day period seem to determine

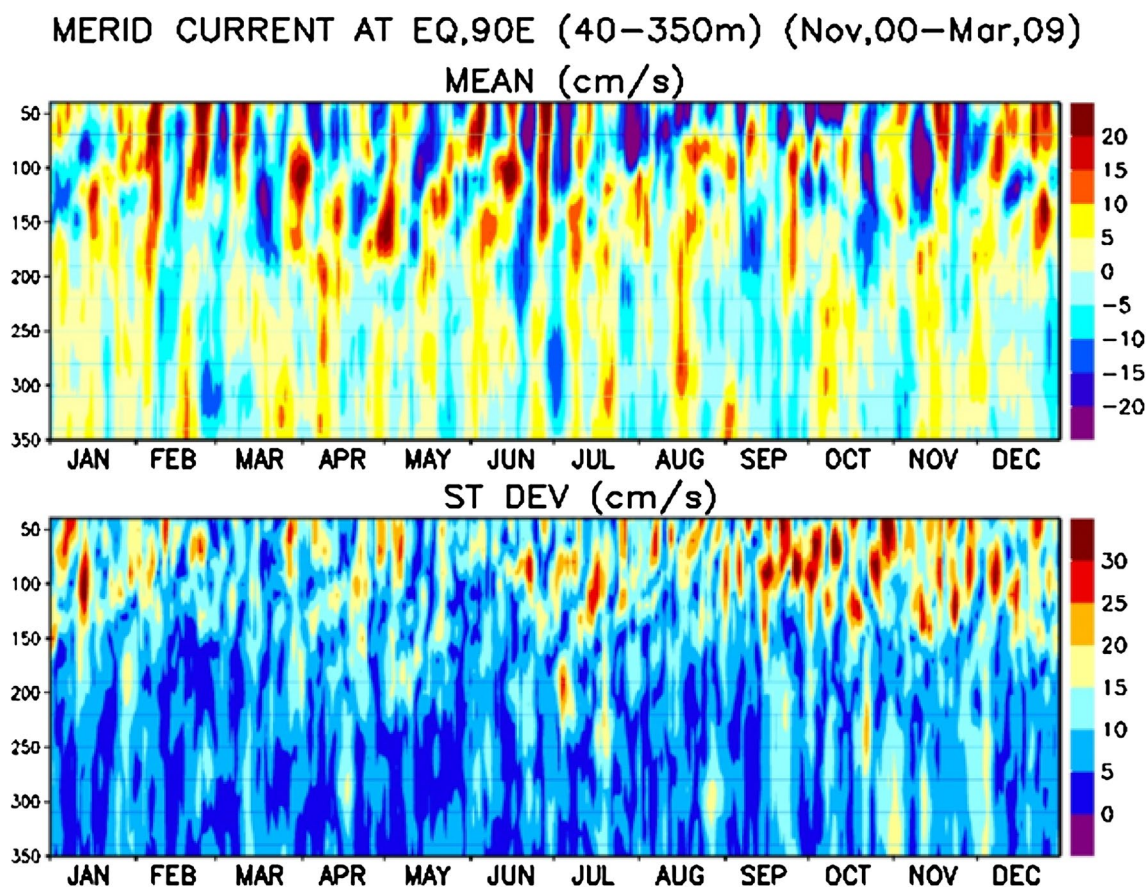


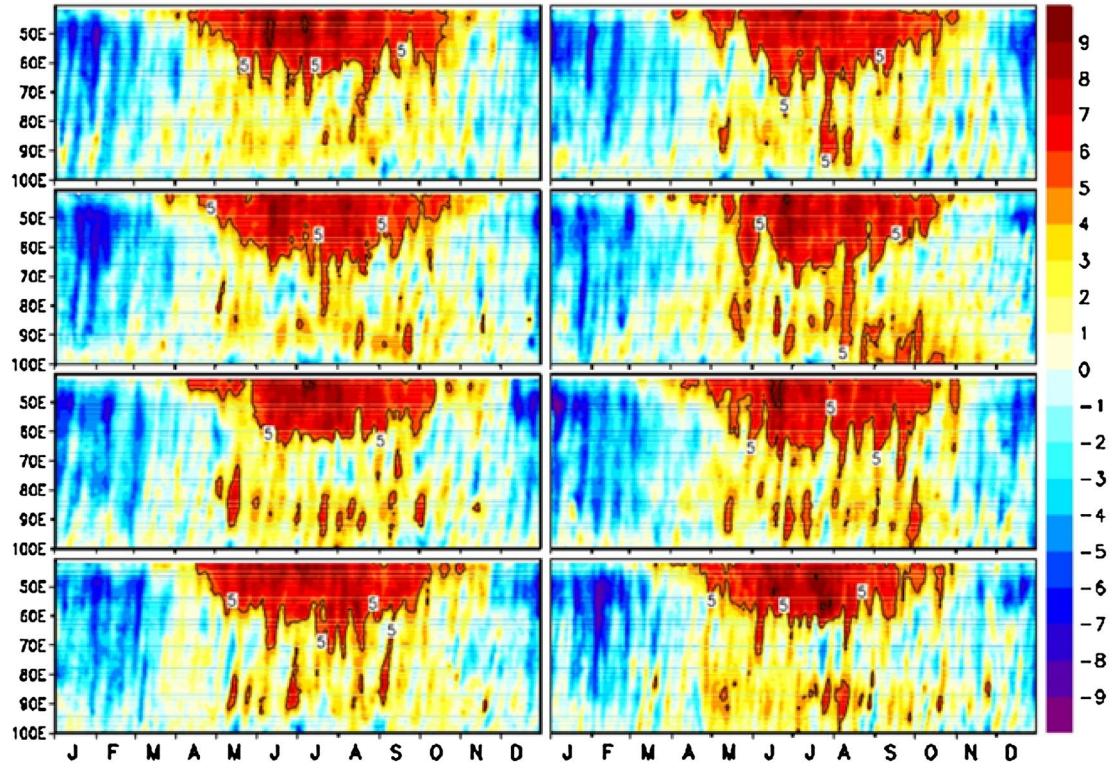
Fig. 3 Annual cycle of the daily climatological mean and standard deviation of the observed ADCP MCs (2000–2009) in the 40–350 m water column at the Equator, 90°E

the active-break cycle of the summer monsoon over the Bay of Bengal (Krishnamurti and Arduay 1980; Sikka and Gadgil 1980). Analysis of NOAA daily outgoing longwave radiation (OLR) and NCEP reanalysis winds at 850 hPa and at higher levels has shown that the quasi-biweekly activity is present throughout the year with varying amplitude (Chatterji and Goswami 2004). Analysis of daily FGGE and OLR data by Chen and Chen (1993) has shown that the quasi-biweekly mode propagates westward along the equator with a speed of 4–5 m/s. The observed inter-annual variability of QuikSCAT MWs along the equator for the individual years 2001–2008 is presented in Fig. 4a. Dominant annual cycle in the MWs is seen along the equator. Due to seasonal reversal of both the monsoons, the amplitude of the annual cycle is more pronounced in the west and it decreases eastward. The seasonal asymmetry is stronger in the west compared to that of in the east. Southerly winds stronger than 5 m/s are mostly confined to westward of 65°E. On the other hand northerly winds stronger than 5 m/s extend further eastward up to 90°E. A clear westward propagation of MWs is also seen throughout the year which is attributed to the westward propagating

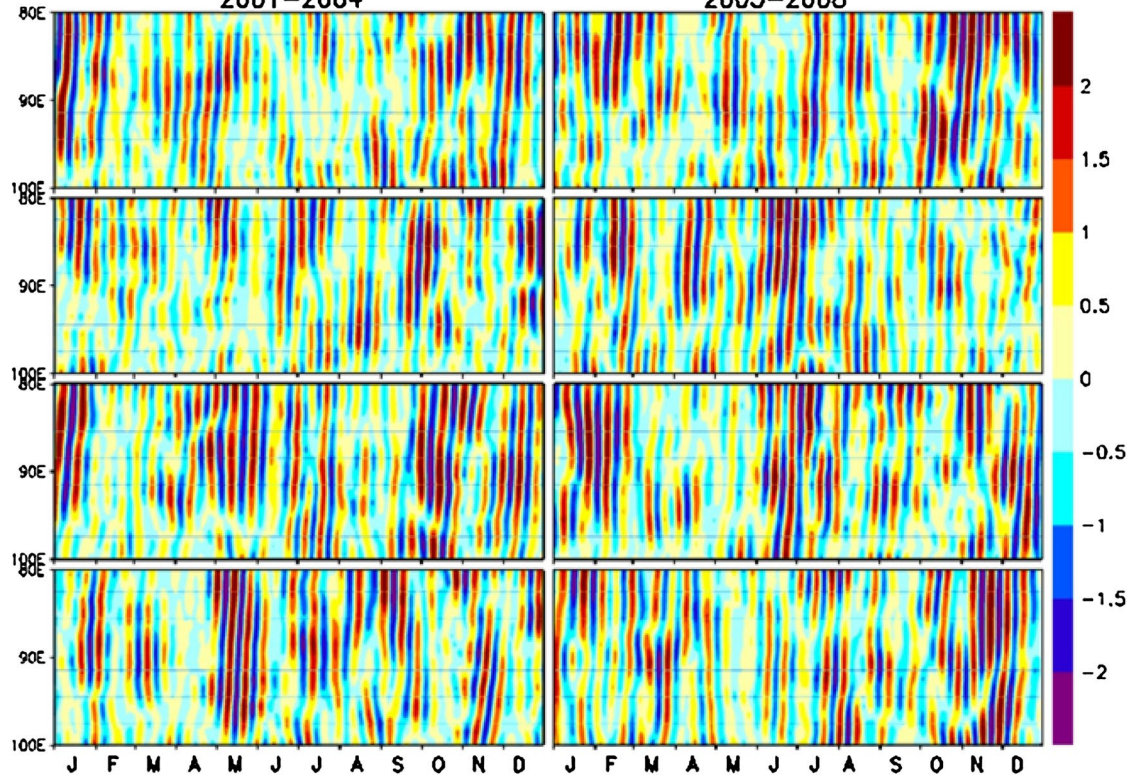
quasi-biweekly mode in the lower troposphere (Krishnamurti and Arduay 1980; Yasunari 1981; Goswami et al. 1998). The most distinct feature of the observed annual cycle is the overriding intraseasonal oscillations throughout the year along the entire equator. The signature of the inter-annual variability is also seen in the eastern EIO where the intraseasonal oscillations are more pronounced only during certain years. At the Equator, 90°E, biweekly mode oscillations in MWs are present throughout the year. These oscillations and their interannual variability are expected to produce a corresponding variability in the observed MC field at the Equator, 90°E.

The 10–20 day bandpass filtered MWs in the longitude band 80°E–100°E is shown in Fig. 4b for the years 2001–2008. The filtered MWs show larger values in the eastern EIO occurring in packets episodically. A great deal of similarity is also seen between the bandpass filtered MW and MC fields. A careful examination also shows a good correspondence between the filtered MW and MC fields (Figs. 2b, 4b) in time. For example, in tune with the MCs, the MWs are also relatively stronger (weaker) during boreal spring in the years 2003 and 2004 (2007 and 2008). During

(a) QSCAT DAILY MERID WINDS (m/s) ALONG THE EQUATOR (40E-100E): 2001-2008
2001-2004 2005-2008



(b) 10-20 DAY BANDPASS FILTERED MERID WINDS (m/s) ALONG EQUATOR (80E-100E)
2001-2004 2005-2008



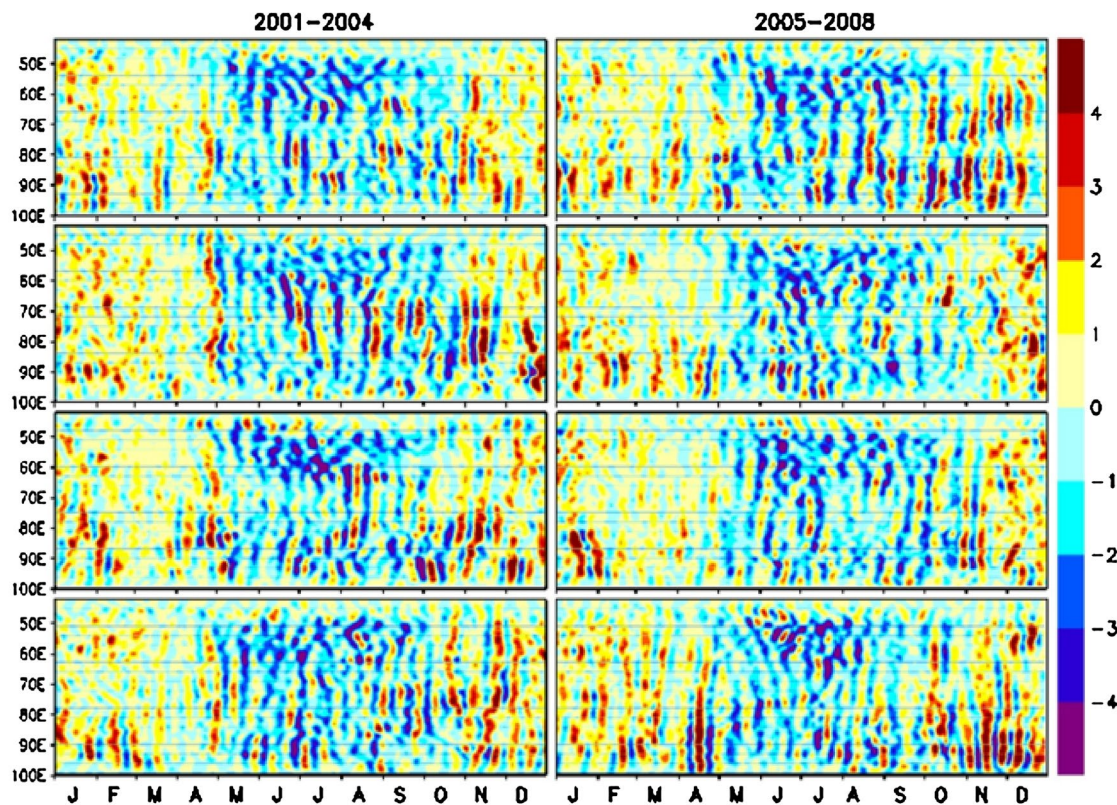
(c) QSCAT 10–20 DAY BP WIND CURL (N/m^3) ALONG EQUATOR (40E–100E): 2001–2008

Fig. 4 continued

◀ **Fig. 4 a** Observed interannual variability of the daily QuikSCAT MWs (m/s) along the equator (average of 2°S – 2°N from 40°E to 100°E) during 2001–2008 (years increasing downward). **b** Observed interannual variability of the 10–20 day bandpass filtered QuikSCAT MWs (m/s) along the equator (2°S – 2°N , 80°E – 100°E) during 2001–2008 (years increasing downward). **c** Interannual variability of the 10–20 day bandpass filtered QuikSCAT wind stress curl ($\text{X E-08 N}/\text{m}^3$) along the equator (average of 2°S – 2°N from 42°E to 100°E) during 2001–2008 (years increasing downward)

the boreal fall season, they are relatively stronger (weaker) during 2001, 2003 and 2005 (2002, 2006 and 2007). During the IOD years 2006 and 2007, the MWs are unusually weaker during the later part of the summer monsoon season and during the boreal fall. Similar episodic nature is also seen in the distribution of bandpass filtered OLR data in the eastern EIO (figure not shown).

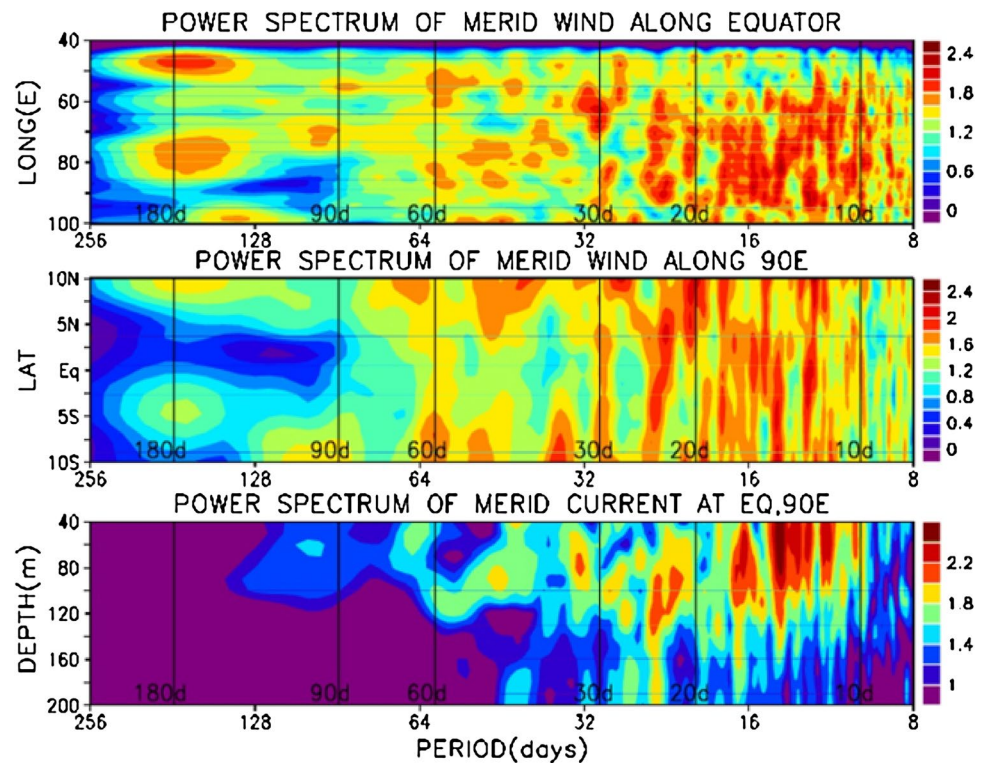
The westward propagating MRG waves are well known to be driven by the MW and the associated surface wind stress curl fields (Blandford 1966; Sengupta et al. 2004). Associated with these quasi-biweekly waves are the north-south reversing MCs—both driven by the westward moving MW and the wind stress curl fields (Ogata et al. 2008).

The distribution of the QuikSCAT wind stress curl along the equator is shown in Fig. 4c to explore its relationship with the MC variability. The wind stress curl data are bandpass filtered for 10–20 days to focus on its quasi-biweekly variability. In general, negative (positive) regime of the wind stress curl values has occurred during boreal summer (boreal winter) seasons. Overriding on this seasonal cycle, strong 10–20 day oscillations are also seen throughout, but more prominently on occasion during both the boreal winter and boreal summer seasons. In close agreement with the westward movement of the MRG waves, westward propagation of these bands is also seen during most of the time although there are exceptions on occasion. During most years these bands are more pronounced during boreal winter, boreal spring and boreal fall with a stronger manifestation over the eastern EIO.

4.2 Relationship between MWs and MCs

The amplitudes of variance preserving power spectra of MWs along the equator (40°E – 100°E), along the 90°E (10°N – 10°S) and MCs at the Equator, 90°E estimated with the respective time series are shown in Fig. 5. Interestingly at

Fig. 5 Amplitudes of variance preserving power spectra of QuikSCAT MWs along the equator (*top panel*), along 90°E (*middle panel*) and JAMSTEC ADCP MCs (40–200 m) at the Equator, 90°E (units are arbitrary and vertical lines indicate the most prominent periods for easy reference)



the semiannual period only the spectra of MWs show peaks while the spectra of MCs do not show any peaks. Along the equator, the two spectral peaks of MWs at this period are seen around 50°E and 80°E. Very low spectral energy of MWs is seen at 90°E. All the three spectra show distinct peaks at 10–20 day and at 20–30 day periods. Along the equator, the MW spectra at these periods are more pronounced in the central and the eastern EIO. Along 90°E, the MW spectra at these periods are equally pronounced over the entire 20 degree latitudinal belt. Consistent with Figs. 2a and 3a, the spectral peaks of the MC field are confined to the uppermost 150 m layer where they are strong and variable. In agreement with the analysis of Masumoto et al. (2005), the spectral peaks of the MC field in the near-surface layer at 10–20 day period are attributed to the corresponding peaks in the MW field driving the MRG waves. The peaks at periods 20–30 days seen in the MC spectral field also more pronounced at deeper depths (80–150 m) are attributed to the MRG waves. The spectra of MCs measured by RCMs at 83°E and at 93°E on the equator also show both quasi-biweekly and 20–30 day peaks at 106 m depth (Sengupta et al. 2004). The OGCM simulations forced by climatological winds by Sengupta et al. (2004) have shown 20–30 day signal in the subsurface layer. Ogata et al. (2008) have also shown 20–70 day signal in the subsurface layer in an OGCM simulation forced by climatological winds. This is attributed to the instability of the seasonally changing current system during boreal fall and early boreal winter in the region southeast of Sri Lanka. The semiannual

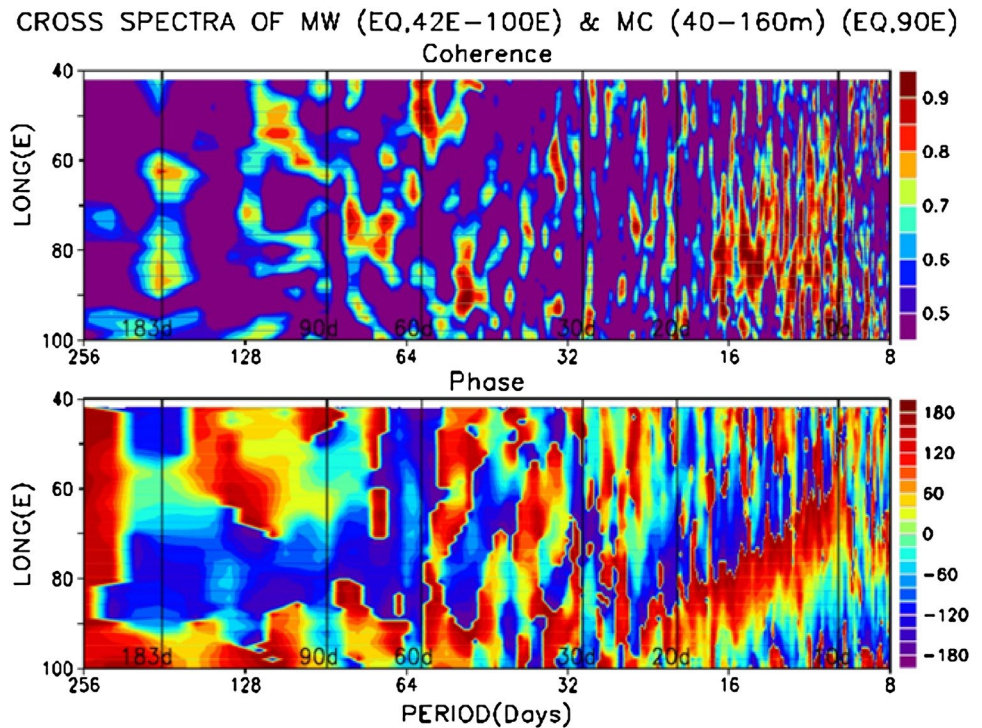
signals are seen in the MW field both in the western and east central EIO and along 90°E at 10°N and 5°S. This suggests that the quasi-biweekly variability in the MC is mostly forced by the corresponding quasi-biweekly variability in the MW field through MRG waves.

The cross spectra between the MWs along the equator and the depth averaged MCs (40–160 m) at the Equator, 90°E through the distributions of coherence and phase are shown in Fig. 6. The coherence between MCs and the MWs is more pronounced along 65°–90°E at the quasi-biweekly period consistent with the modeling results of Sengupta et al. (2004) and of Ogata et al. (2008). The signal is more pronounced in the central and eastern EIO. The phase difference at 90°E translates to about 2 days implying that at quasi-biweekly period the MC responds to local MW wind forcing in just about 2 days. Sengupta et al. (2004) have also found in their model simulation that the quasi-biweekly oscillation is absent in the seasonal run, demonstrating that it is forced by the intraseasonal wind variability and not by dynamic instability.

5 Relationship between MCs and barrier layer thickness

A relationship between the ZC at this location and BLT at a nearby location (1.5°S, 90°E) is noticed in the time scale

Fig. 6 Coherence (*top panel* in arbitrary units) between QuikSCAT MWs along the equator (42°E–100°E) and JAMSTEC ADCP MCs (40–160 m) at the Equator, 90°E and phase (*bottom panel* in degrees) (*vertical lines* indicate the most prominent periods for easy reference)



of 30–60 days (Rao et al. 2015). The time series data of BLT (Fig. 13a in Rao et al. 2015) have also shown high frequency variability. Hence the relationship between the BLT and the MC is examined in the time scale of 10–20 days. In general, the temporal correspondence of these two time series both in amplitude and in phase is quite high indicating a strong relationship between the two. The MC lags the BLT by about 4 days suggesting that this is the response time for the MC to build up under the MW forcing when the mixed layer thins due to increase in BLT. The cross spectra in terms of coherence and phase between BLT and the depth averaged (40–100 m) MC is shown in Fig. 7b. The coherence between BLT and MC is quite pronounced at 10–20 day period. In addition, strong peaks also occur in the temporal range of 20–60 days and at other higher periods. The phases corresponding to the coherence peaks at 12, 14 and 18 days also suggest that the MC lags BLT by about 4 days.

6 Upwelling/downwelling in the near off-equatorial region associated with the MRG waves

The signature of upwelling/downwelling is best captured by the vertical fluctuations of density field in the pycnocline. The daily vertical profiles of temperature and salinity data recorded at the TRITON buoy location 1.5°S, 90°E for nearly 6 years offer an excellent opportunity to

characterize the upwelling/downwelling cycles in the pycnocline associated with the MRG waves. The amplitude of variance preserving power spectral distribution of the density field in the 40–200 m water column estimated from vertical temperature and salinity profiles recorded at the TRITON buoy location is shown in Fig. 8. A distinct band of spectral peaks is seen in the core of the pycnocline region (80–120 m) both at the semiannual and intraseasonal periods. The semiannual peak alone shows a tendency for downward penetration. Hase et al. (2008) have examined the time series of temperature and salinity measurements collected by this TRITON buoy moored in the eastern EIO. Their spectral analysis indicates that the dominant temperature signals in the thermocline shows semiannual periodicity. Consistent with the earlier studies, at 100 m depth the energetic intraseasonal variability is dominant, with periods of 13 and 34 days for temperature attributed to MRG waves and intraseasonal variability forced by the atmosphere respectively. Previous investigators (Kindle and Thompson 1989; Sengupta et al. 2001; Ogata et al. 2008) have shown in their model simulations driven by monthly mean winds that the instability as the prime factor producing variability in the simulated flow patterns with periods of 20–70 days. The density fluctuations in the pycnocline at quasi-biweekly period are attributed to the occurrence of off equatorial upwelling/downwelling cycles (Gill 1982; Sengupta et al. 2004; Ogata et al. 2008) associated with westward propagating equatorially trapped MRG waves.

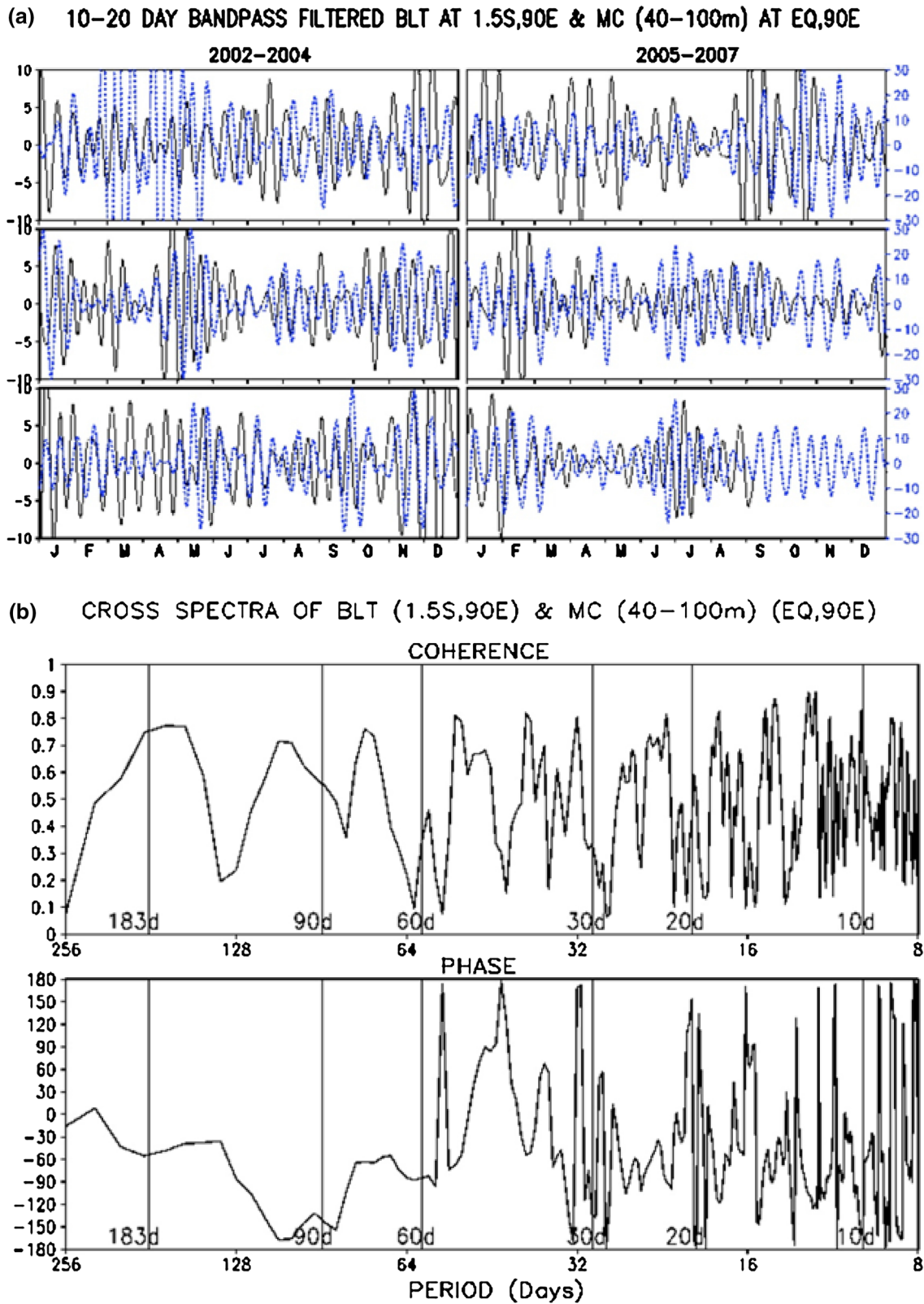
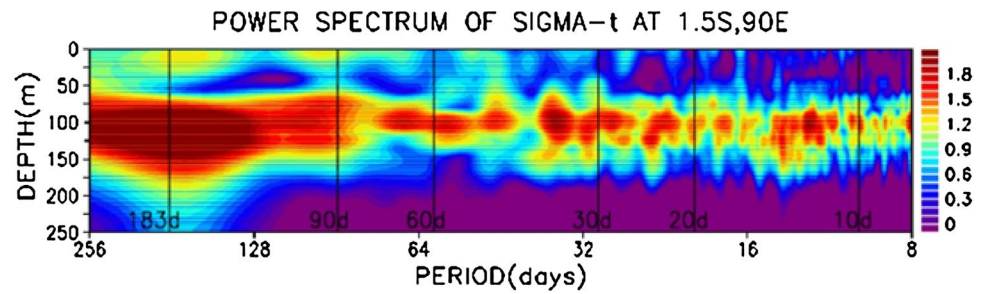


Fig. 7 a Daily evolution of 10–20 day bandpassed vertically averaged MC (cm/s) (40–100 m) at the Equator, 90°E (blue line) and BLT (m) at 1.5°S, 90°E (black line) during 2002–2007 (years increasing downward). **b** Coherence (top panel in arbitrary units) and phase

(bottom panel in degrees) between BLT at 1.5°S, 90°E and MC (40–100 m) at Equator, 90°E (vertical lines indicate the most prominent periods for easy reference)

Fig. 8 Amplitude of variance preserving power spectrum of sigma-t at 1.5°S, 90°E in the upper 250 m water column (units are arbitrary. The density data are de-meaned and spectral estimates are scaled up by 1000 for plotting purpose. Vertical lines represent the most prominent periods for reference)



In the OGCM simulations, the quasi-biweekly westward propagating equatorially trapped MRG waves are associated with fluctuating upwelling/downwelling cycles with amplitude of 2–3 m/day in the pycnocline 200–300 km on either side of the equator, connected by cross-equatorial meridional flow (Sengupta et al. 2004; Ogata et al. 2008). To validate this modeling result, the vertical fluctuations of isopycnals in the core region of the pycnocline are examined from the available TRITON moored time series CTD data recorded at 1.5°S, 90°E for the typical year 2003 (Fig. 9a). The pycnocline shows a strong semiannual variability with superposed fluctuations on intraseasonal time scale. The model simulations show southward (northward) flow in association with downwelling (upwelling) south of the equator consistent with the convergence/divergence associated with westward propagating MRG waves. Observational evidence for this phenomenon is shown by overlaying both the MC and isopycnal fields together. A careful examination of the pycnocline region in this figure shows the co-occurrence of southward (northward) flow and downward (upward) movement of pycnocline in general confirming the validity of the model results. Thus the co-availability of time series measurements of both ADCP data at the Equator, 90°E and TRITON CTD data at 1.5°S, 90°E has provided an excellent opportunity to validate the model results in the real ocean for the first time. The cross spectra in terms of coherence and phase between sigma-t and depth averaged (40–100 m) MC fields (Fig. 9b) also show prominent peaks at the 10–20 day period. The phase corresponding to the coherence peaks in the 10–20 day period at 12, 14 and 16 days also suggest that the sigma-t lags MC by about 3 days which corresponds to a phase shift of 90°.

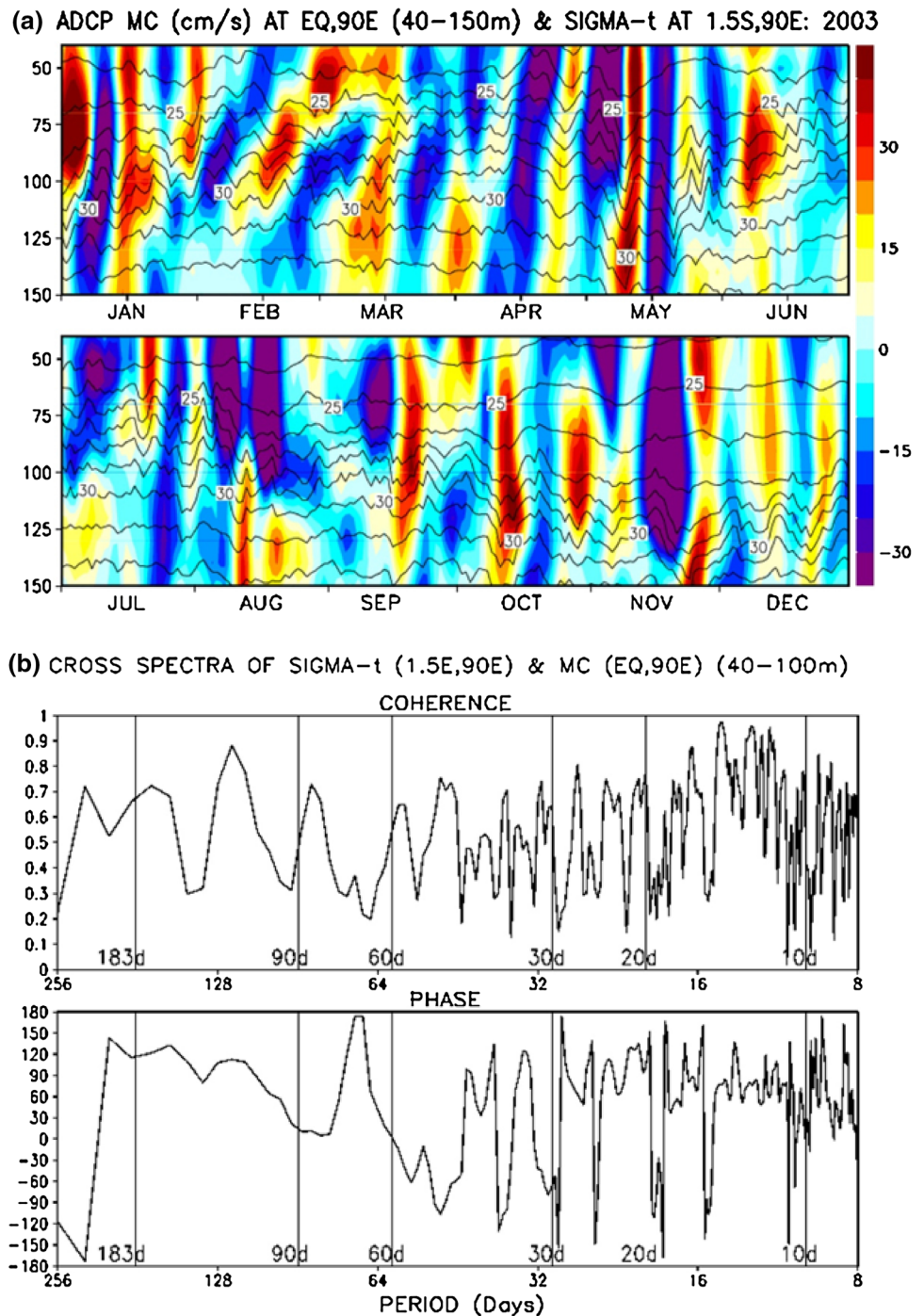
To capture the correspondence between the upwelling/downwelling cycles and the associated meridional flow, the 10–20 day bandpass filtered MWs in the eastern EIO (80°–100°E), MCs (at the Equator, 90°E) and the density (shown as sigma-t at 1.5°S, 90°E) in the 40–150 m layer for a representative year 2003 are shown in Fig. 10. Large co-variability occurs as packets in all these three parameters that shows excellent temporal coherence over an annual cycle. Current meter data from two locations on the equator have also shown that packets of MRG waves

propagate westward along the equatorial wave guide (Sengupta et al. 2004). All these three parameters show strong signatures during boreal winter, boreal spring and boreal fall indicating a strong relationship among the three independent time series. The packets of strong MWs phase velocity show westward propagation throughout the year. The packets of strong MCs generally show upward phase propagation consistent with the results of Sengupta et al. (2004). However, the energy of the quasi-biweekly MRG waves at a given longitude is due to both local forcing and energy arriving from the west as MRG waves have eastward group velocity (Sengupta et al. 2004; Ogata et al. 2008). The quasi-biweekly oscillations of surface MWs trigger quasi-biweekly MRG waves in the EIO. The packets of relatively stronger density fluctuations at 1.5°S, 90°E more prominently seen in the region where the pycnocline is relatively sharper also show upward propagation. These density fluctuations are attributed to upwelling/downwelling cycles associated with the westward propagating MRG waves. The quasi-biweekly wave is associated with fluctuating upwelling/downwelling cycles in the EIO away from the equator connected by cross-equatorial meridional flow. Other years also show similar characteristics with some minor differences.

7 Relationship between SST and MRG waves

Submonthly intraseasonal oscillations are well known to cause significant SST variability on 10–30 day time scale in the EIO (Han et al. 2006). However, no study has reported that MRG waves can also show up their signatures on the westward propagation of SST along the equator. The 10–20 day bandpass filtered SST along the equator is examined (Fig. 11a) to assess the influence of westward propagating MW and the associated MRG wave fields on its evolution. Interestingly distinct quasi-biweekly variability is also seen in SST almost throughout the year with relatively larger amplitudes during boreal fall and boreal winter. In general, the amplitudes are relatively weaker during summer monsoon season. Although there are a few exceptions, it is interesting to note the westward propagation of

Fig. 9 **a** Observed annual cycle of MC at the Equator, 90°E and sigma-t contours at 1.5°S, 90°E in the 40–150 m water column during 2003. **b** Coherence (*top panel* in arbitrary units) and phase (*bottom panel* in degrees) between sigma-t at 1.5°S, 90°E and MC averaged over 40–100 m water column at Equator, 90°E (*vertical lines* represent the most prominent periods for easy reference)



this quasi-biweekly variability in the filtered SST field with phase speed resembling that of the MRG waves episodically in the summer monsoon season during most years. In order to establish that this westward propagation is caused by the MRG waves, the corresponding quasi-biweekly variability in the 10–20 day filtered OLR and surface net heat flux data—two thermodynamic parameters which control SST are shown along the equator during the summer

monsoon season of 2004 (Fig. 11b). A quasi-biweekly variability with coherent structures in both OLR and surface net heat flux fields propagates eastward throughout the summer monsoon season while the quasi-biweekly variability in the SST shows westward propagation. Thus it is clear that the westward propagating quasi-biweekly SST variability does not appear to be coupled with any thermodynamic process but driven by the westward propagating MRG waves.

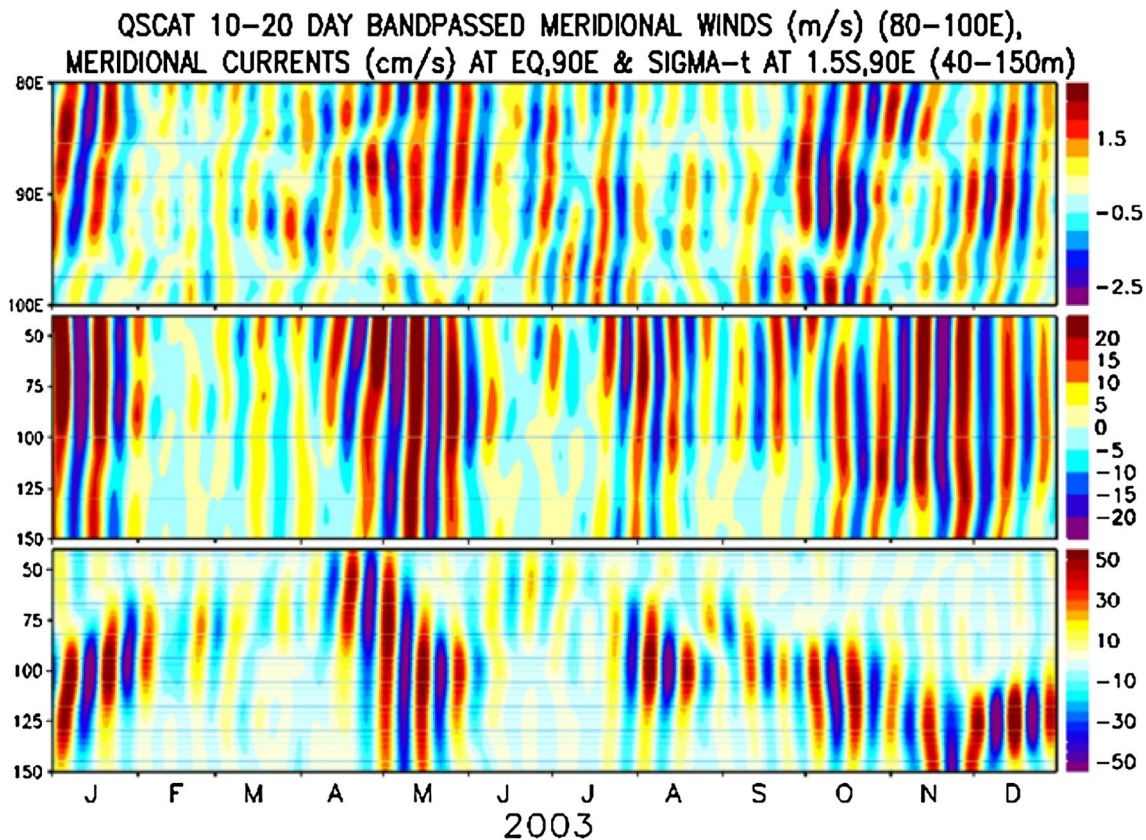


Fig. 10 10–20 day bandpass filtered MWs along 80°–100°E, MCs at Equator, 90°E and sigma-t at 1.5°S, 90°E in the 40–150 m water column during 2003

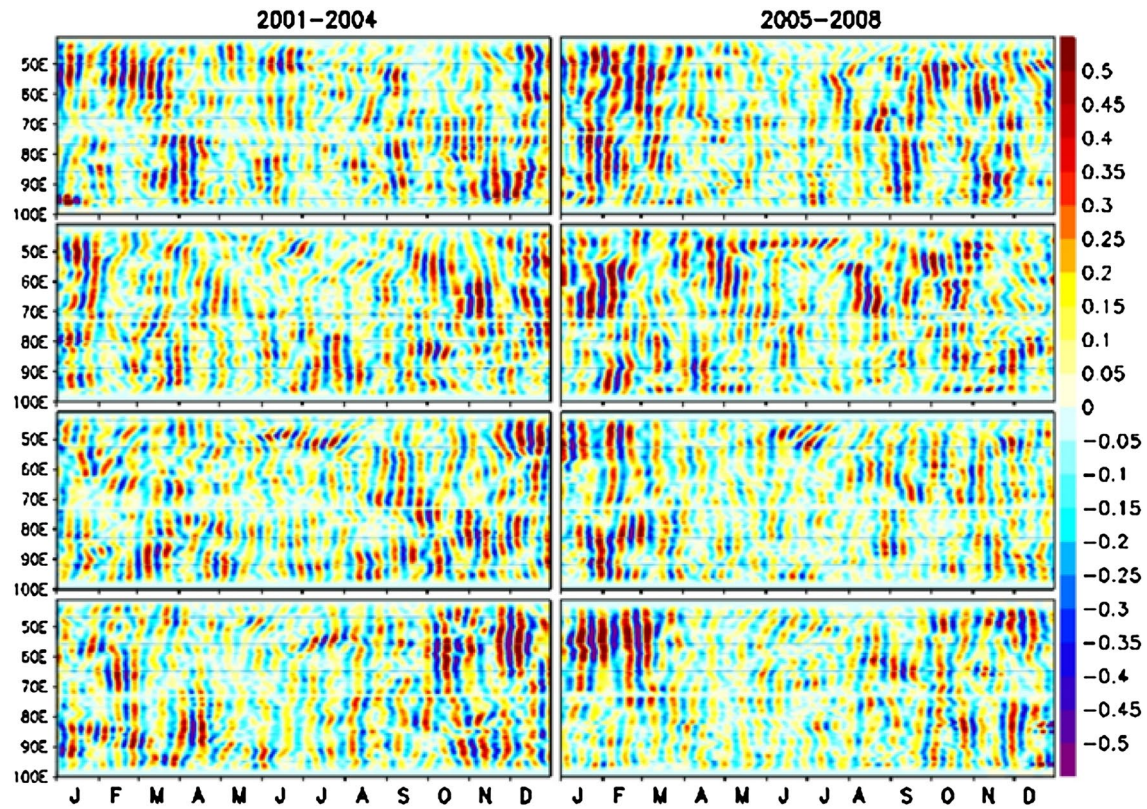
8 Summary

The mean distribution of MCs does not show any clear seasonality in the 40–350 m water column. Instead, a complex vertical structure of alternate bands of northward and southward flowing currents at high frequency (quasi-biweekly) is seen throughout this water column. The amplitude of the variability tends to be large during boreal spring and boreal fall in tune with the depression of the pycnocline associated with the Wyrtki jets. Relatively larger amplitudes are seen in the uppermost 150–200 m layer compared to the below layers. A careful examination reveals interannual modulation of this quasi-biweekly variability in the MC field. The observed sharp differences in the MCs between years appear to be determined by the strengths of both MWs and BLT. The most distinct feature of the observed annual cycle of the MW field is the overriding intraseasonal oscillations along the entire equator throughout the year. A clear westward propagation of MWs is also seen throughout the year which is attributed to the westward propagating quasi-biweekly mode in the lower troposphere. The bandpass filtered MWs in the eastern EIO show large values occurring

in packets episodically. A great deal of temporal correspondence is seen between the bandpass filtered MW and MC fields. The westward propagating MRG waves are well known to be driven by the MWs and the associated surface wind stress curl field. Overriding the seasonal cycle, strong 10–20 day oscillations are seen throughout in the surface wind stress curl field. The atmospheric quasi-biweekly mode resonately forces quasi-biweekly MRG waves in the eastern EIO and the MCs associated with these waves also accordingly show the quasi-biweekly variability.

The power spectra of MWs and MCs show distinct peaks at 10–20 day and at 20–30 day periods. Along the equator, the spectra are more pronounced in the central and the eastern EIO. Along 90°E, the spectra are equally pronounced between 10°N and 10°S. The spectral peaks of the MC field in the near-surface layer are attributed to the corresponding peaks in the MW field that drives the MRG waves. The spectral peaks at periods 20–30 days at deeper depths (80–150 m) are also attributed to MRG (Yanai) waves. The coherence between depth integrated (40–160 m) MC at the Equator, 90°E and the MW along 65°–90°E is more pronounced at the quasi-biweekly period. The phase difference

(a) 10–20 DAY BANDPASS FILTERED TRMM TMI DAILY SST ALONG EQUATOR: 2001–2008



(b) 10–20 DAY BANDPASSED NOAA OLR, WHOI QNET & TMI SST ALONG EQUATOR

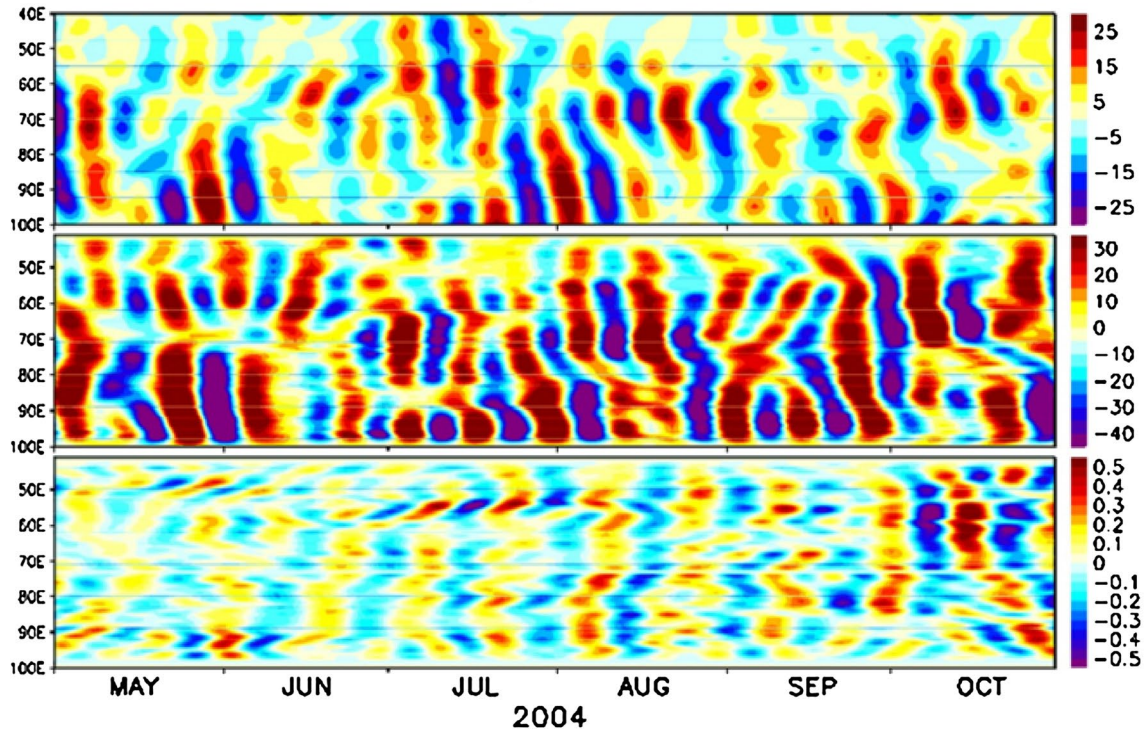


Fig. 11 a 10–20 day bandpass filtered TRMM TMI SST ($^{\circ}\text{C}$) along the equator during the years 2001–2008 (years increasing downward). b 10–20 day bandpass filtered NOAA OLR (W/m^2) (top panel),

WHOI surface net heat flux (W/m^2) (middle panel) and TRMM TMI SST ($^{\circ}\text{C}$) (bottom panel) along the equator (40°E – 100°E) during the summer monsoon season of 2004

at 90°E translates to about 2 days implying that at the quasi-biweekly period the MC responds to local MW wind forcing in just about 2 days.

The cross spectra between BLT and the depth averaged (40–100 m) MC in terms of amplitude and phase indicate a strong relationship between the two at quasi-biweekly time scale. The MC lags the BLT by about 4 days suggesting that this is the response time for the MC to build up under the MW forcing when the mixed layer thins due to increase in BLT. A distinct band of spectral peaks is also seen in the core region of the pycnocline (80–120 m) both at the semiannual and intraseasonal periods. The semiannual peak alone shows a tendency for downward penetration. The peaks at quasi-biweekly period and at 20–90 day period are attributed to MRG waves and intraseasonal variability forced by the atmosphere respectively. The density fluctuations in the pycnocline at quasi-biweekly period are attributed to the occurrence of upwelling/downwelling cycles associated with westward propagating MRG waves. Large co-variability occurs in packets of the bandpass filtered MW, MC and density fields that shows excellent temporal correspondence over an annual cycle. The packets of relatively stronger density fluctuations at 1.5°S, 90°E are more prominently seen in the region where the pycnocline is relatively sharper. These density fluctuations are attributed to upwelling/downwelling cycles associated with the westward propagating MRG waves triggered by the quasi-biweekly MWs. A suggestion of westward propagation of quasi-biweekly variability in SST with phase speed resembling that of the MRG waves is also seen episodically in the summer monsoon season during most years. Future analysis of long time series measurements made through the deployment of moored vertical arrays in its full measure under RAMA observational initiative in the TIO and improved models would provide answers to questions that remained unanswered in this study.

Acknowledgments Highest appreciation is placed on record for the excellent compilation by several persons and organizations of all the data sets utilized in this study. JAMSTEC is responsible for the deployment of ADCP and TRITON CTD moorings in the eastern EIO. The Graphics were generated with GrADS. The encouragement and the facilities provided by the Director General, JAMSTEC are gratefully appreciated. This research was carried out while the first author held a Visiting Senior Scientist position at JAMSTEC with the support of JEPP (Japan Earth Observation Promotion Program) of MEXT (Ministry of Education, Culture, Sports, Science and Technology), Japan.

References

- Akima H (1970) A new method of interpolation and smooth curve fitting based on local procedures. *J Assoc Comput Mech* 17:589–602
- Blandford RR (1966) Mixed gravity-Rossby waves in the ocean. *Deep-Sea Res* 13:941–961
- Bleck R (2002) An oceanic general circulation model framed in hybrid isopycnic-Cartesian coordinates. *Ocean Model* 4:55–88
- Chatterji P, Goswami BN (2004) Structure, genesis and scale selection of the tropical quasi-biweekly mode. *Q J R Meteorol Soc* 130(599):1171–1194
- Chen TC, Chen JM (1993) The 10–20 day mode of the 1979 Indian Monsoon: its relation with the time variation of monsoon rainfall. *Mon Weather Rev* 121:2465–2482
- Duchon CE (1979) Lanczos filter in one and two dimensions. *J Appl Meteorol* 18:1016–1022
- Gill AE (1982) *Atmosphere-ocean dynamics*. Academic, San Diego
- Goswami BN, Sengupta D, Kumar S (1998) Intraseasonal oscillations and interannual variability of surface winds over the Indian monsoon region. *Proc Ind Acad Sci* 107(1):45–64
- Halkides DJ, Han W, Lee T, Masumoto Y (2007) Effects of sub-seasonal variability on seasonal-to-interannual Indian Ocean meridional heat transport. *Geophys Res Lett* 34:L12605. doi:10.1029/2007GL030150
- Han W, Liu WT, Lin J (2006) Impact of submonthly oscillations on sea surface temperature of the tropical Indian Ocean. *Geophys Res Lett* 33:L03609. doi:10.1029/2005GL025082
- Hase H, Masumoto Y, Kuroda Y, Mizuno K (2008) Semiannual variability in temperature and salinity observed by Triangle Tans-Ocean Buoy Network (TRITON) buoys in the eastern tropical Indian Ocean. *J Geophys Res* 113:C01016. doi:10.1029/2006JC004026
- Hino M (1977) *Spectral analysis*. Asakura-SyoTen, Tokyo (in Japanese)
- Johnson ES, Bonjean F, Lagerloef GSE, Gunn JT, Mitchum GT (2007) Validation and error analysis of OSCAR sea surface currents. *J Ocean Atmos Technol* 24(4):688–701
- Kindle JC, Thompson JD (1989) The 26 and 30 day oscillation in the western Indian Ocean: model results. *J Geophys Res* 94:4721–4736
- Knox R (1976) On a long series of measurements of Indian Ocean equatorial currents near Addu Atoll. *Deep Sea Res* 23:211–221
- Krishnamurti TN, Arduinay P (1980) The 10 to 20 day westward propagating mode and “breaks in the monsoons”. *Tellus* 32:15–26
- Kuroda Y (2002) TRITON: Present status and future plan. JAMSTEC Tech. Rep. TOCS 5, Japan Marine Science and Technology Center, Yokosuka, Japan
- Lagerloef GSE, Mitchum GT, Lukas R, Niiler PP (1999) Tropical Pacific near surface currents estimated from altimeter, wind and drifter data. *J Geophys Res* 104:23313–23326
- Loschnigg J, Webster P (2000) A coupled ocean-atmosphere system of SST modulation for the Indian Ocean. *J Clim* 13:3342–3360
- Luyten JR, Roemmich DH (1982) Equatorial currents at semiannual period in the Indian Ocean. *J Phys Oceanogr* 12:406–413
- Masumoto Y, Hase H, Kuroda Y, Matsuura H, Takeuchi K (2005) Intraseasonal variability in the upper layer currents observed in the eastern equatorial Indian Ocean. *Geophys Res Lett* 32:L02607. doi:10.1029/2004GL021896
- Matsuno T (1966) Quasi-geostrophic motions in the equatorial area. *J Meteorol Soc Jpn* 44:25–43
- McPhaden MJ (1982) Variability in the central equatorial Indian Ocean: I. Ocean dynamics. *J Mar Res* 40:157–176
- Miyama T, McCreary JP, Jensen TG, Loschnigg J, Godfrey S, Ishida A (2003) Structure and dynamics of the Indian Ocean cross-equatorial cell. *Deep Sea Res Part II* 50:2023–2047
- Miyama T, McCreary JP, Sengupta D, Senan R (2006) Dynamics of quasi-biweekly oscillations in the equatorial Indian Ocean. *J Phys Oceanogr* 36:827–846

- Murty VSN, Sarma MSS, Suryanarayana A, Sengupta D, Unnikrishnan AS, Fernando V, Almeida A, Khalap S, Sardar A, Somasundar K, Ravichandran M (2006) Indian moorings: deep-sea current meter moorings in eastern equatorial Indian Ocean. CLIVAR Exchanges, No. 11 (4), International CLIVAR Project Office, Southampton, UK, pp 5–8
- Ogata T, Sasaki H, Murty VSN, Sarma MSS, Masumoto Y (2008) Intraseasonal meridional current variability in the eastern equatorial Indian Ocean. *J Geophys Res* 113:C07037. doi:[10.1029/2007/JC004331](https://doi.org/10.1029/2007/JC004331)
- Qu T, Meyers G (2005) Seasonal variation of barrier layer in the southeastern tropical Indian Ocean. *J Geophys Res*. doi:[10.1029/2004JC002816](https://doi.org/10.1029/2004JC002816)
- Rao RR, Girish Kumar MS, Ravichandran M, Sathesh Kumar S (2009) Atlas of the tropical Indian Ocean from satellite observations, volume I: sea surface wind vectors and wind stress curl, Indian National Centre for Ocean Information Services (INCOIS), Hyderabad, India. ISBN: 978-81-8424-326-0
- Rao RR, Horii T, Masumoto Y, Mizuno K (2015) Observed variability in the upper layers at the Equator, 90°E in the Indian Ocean during 2001–2008, 1: zonal currents. *Clim Dyn*
- Reppin J, Schott F, Fischer J, Quadfasel D (1999) Equatorial currents and transports in the upper central Indian Ocean. *J Geophys Res* 104:15495–15514
- Reverdin G, Luyten J (1986) Near-surface meanders in the equatorial Indian Ocean. *J Phys Oceanogr* 16:1088–1100
- Schott F, McCreary JP (2001) The monsoon circulation of the Indian Ocean. *Prog Oceanogr* 51:1–123
- Schott F, Reppin J, Fischer J, Quadfasel D (1994) Currents and transports of the monsoon current south of Sri Lanka. *J Geophys Res* 99:25127–25141
- Schott FA, McCreary JP, Johnson GC (2004) Shallow over-turning circulations of the tropical-subtropical oceans. In: Wang C, Xie SP, Carton JA (eds) *Earth's climate: the ocean–atmosphere interaction*, geophysical monograph series, vol 147. AGU, Washington, pp 261–304
- Schott FA, Xie SP, McCreary JP (2009) Indian Ocean circulation and climate variability. *Rev Geophys* 47:RG1002. doi:[10.1029/2007RG000245](https://doi.org/10.1029/2007RG000245)
- Sengupta D, Senan R, Goswami BN (2001) Origin of intraseasonal variability of circulation in the tropical central Indian Ocean. *Geophys Res Lett* 28(7):1267–1270
- Sengupta D, Senan R, Murty VSN, Fernando V (2004) A quasi-biweekly mode in the equatorial Indian Ocean. *J Geophys Res* 109:C10003. doi:[10.1029/2004JC002329](https://doi.org/10.1029/2004JC002329)
- Shikhakolli R, Sharma R, Basu S, Gohil BS, Sarkar A, Prasad KVS (2013) Evaluation of OSCAR ocean surface current product in the tropical Indian Ocean using in situ data. *J Earth Syst Sci* 122(1):187–199
- Sikka DR, Gadgil S (1980) On the maximum cloud zone and the ITCZ over Indian longitudes during the southwest monsoon. *Mon Weather Rev* 108:1840–1853
- Thompson B, Gnanaseelan C, Salvekar PS (2006) Variability in the Indian Ocean circulation and salinity and its impact on SST anomalies during dipole events. *J Mar Res* 64:853–880
- Tsai PTH, O'Brien JJ, Luther ME (1992) The 26-day oscillation observed in the satellite sea surface temperature measurements in the equatorial western Indian Ocean. *J Geophys Res* 97:9605–9618
- Waliser DE, Murtugudde R, Lukas L (2004) Indo-Pacific Ocean response to atmospheric intraseasonal variability. Part II: boreal summer and the intraseasonal oscillation. *J Geophys Res* 109:C03030. doi:[10.1029/2003JC002002](https://doi.org/10.1029/2003JC002002)
- Wentz FJ, Ashcroft PD, Gentemann CL (2001) Post-launch calibration of the TRMM microwave imager. *IEEE Trans Geosci Remote Sens* 39(2):415–422
- Wunsch C, Gill AE (1976) Observations of equatorially trapped waves in Pacific sea level variations. *Deep Sea Res* 23:371–390
- Wyrtki K (1973) An equatorial jet in the Indian Ocean. *Science* 181:262–264
- Yasunari T (1981) Structure of an Indian summer monsoon system with around 40 day period. *J Meteorol Soc Jpn* 59:336–354